# Imaging a $^6$Li Atom in an Optical Tweezer 2000 Times with Λ-Enhanced Gray Molasses

Karl N. Blodgett,[1] David Peana,[1] Saumitra S. Phatak,[2] Lane M. Terry,[1]
Maria Paula Montes,[2] and Jonathan D. Hood[1,2,*]
[1]Department of Chemistry, Purdue University, West Lafayette, Indiana 47907, USA
[2]Department of Physics and Astronomy, Purdue University, West Lafayette, Indiana 47907, USA

(Received 4 May 2023; accepted 31 July 2023; published 21 August 2023)

We have imaged lithium-6 thousands of times in an optical tweezer using Λ-enhanced gray molasses cooling light. Despite being the lightest alkali metal, with a recoil temperature of 3.5 μK, we achieve an imaging survival of 0.999 50(2), which sets the new benchmark for low-loss imaging of neutral atoms in optical tweezers. Lithium is loaded directly from a magneto-optical trap into a tweezer with an enhanced loading rate of 0.7. We cool the atom to 70 μK and present a new cooling model that accurately predicts steady-state temperature and scattering rate in the tweezer. These results pave the way for ground state preparation of lithium en route to the assembly of the LiCs molecule in its ground state.

DOI: 10.1103/PhysRevLett.131.083001

Optical tweezers are a dynamic platform for manipulating ultracold atoms and molecules in a variety of applications, including few-body physics with neutral atoms [1,2], long-range interactions with arrays of Rydberg atoms [3,4], and atom-by-atom molecular assembly and dipolar interaction [5–10]. The fluorescence of a single atom can be imaged with high fidelity, allowing for single site control and rearrangement of a partially filled array into arbitrary, low entropy configurations [11,12].

Imaging survival probability affects gate fidelity readout with Rydberg atoms, and is a limiting factor in molecular assembly and the production of defect-free arrays [11,13]. Tweezer-trapped alkali atoms have been conventionally imaged with polarization gradient (PG) cooling light [1,14] with survival probability per image of approximately 0.98. Recently, Λ-enhanced gray molasses (Λ-GM) cooling [15] has been used in tandem with resonant scattering light to image $^{39}$K with a survival rate exceeding 0.99 [16]. Λ-GM combines principles from gray molasses [17,18], where dark states are created due to polarization selection rules, with electromagnetically induced transparency (EIT) cooling [19–21], where dark states are created by two lasers that are two-photon resonant between two hyperfine ground states. The narrow optical transition lines of alkaline-earth atoms (AEAs) make them suitable for new cooling techniques, with which the survival rate has been pushed to 0.999 32(8), the current benchmark for low-loss neutral atom imaging [22].

In this Letter, we demonstrate imaging of lithium in an optical tweezer using Λ-enhanced GM light with a survival probability of 0.999 50(2) [Fig. 1(a)]. This represents an order of magnitude improvement over survival probability in other alkali atoms, and even surpasses the best results with narrowline AEAs. The 0 and 1 atom cases are distinguished with a fidelity of 0.999 7(2), which comes as an order of magnitude improvement over existing lithium single atom imaging techniques [23–26].

We develop a numerical model based on the master equation that accurately predicts the steady-state temperature and scattering rate in the tweezer. As shown in Fig. 1(d), motional energy is removed by Raman coupling from a dark state to a bright state with one less motional quanta, followed by optical pumping back to a dark state. Our model suggests that this scheme may be used to cool trapped lithium atoms along one motional axis at a time, similar to existing motional cooling techniques but with a marked reduction in experimental complexity. This would lay the groundwork for the formation of the LiCs molecule in its ground state, which, with the largest dipole moment (5.5 Debye) of any bialkali molecule, is a promising candidate for molecule-based quantum gates.

The experiment begins with using the D2 line to load a 3D magneto-optical trap (MOT) of approximately $10^5$ $^6$Li atoms in 100 ms in the science region of our vacuum chamber (Fig. 2). Since loading optical tweezers requires relatively few atoms, we use the radial decay of the quadrupole magnetic field from the MOT coils, rather than a conventional tapered-coil design, for our Zeeman field.

To initiate tweezer loading, the 3D MOT is overlapped with a 1064 nm tweezer beam that is generated from a low-noise, high-power fiber laser. Magnetic fields are switched off and 3 ms of Λ-GM is applied to the D1 line of the atomic cloud, cooling the atoms to subdoppler temperatures of 100 μK. The optimum free-space cooling conditions are a two-photon detuning $\Delta = 0$ MHz, single-photon detuning $\delta = 30$ MHz, $I_{\mathrm{rep}}/I_{\mathrm{cool}} = 1/10$, and $I/I_{\mathrm{sat}} = 15.0$. The repumper light is generated as a coherent sideband of the cooler light with an electro-optic modulator. We observe the onset of tweezer loading at a trap depth of $U/k_B \approx 0.3$ mK, and saturation to an enhanced loading rate of 0.7 at 1.2 mK [Fig. 3(b)].

 © 2023 American Physical Society

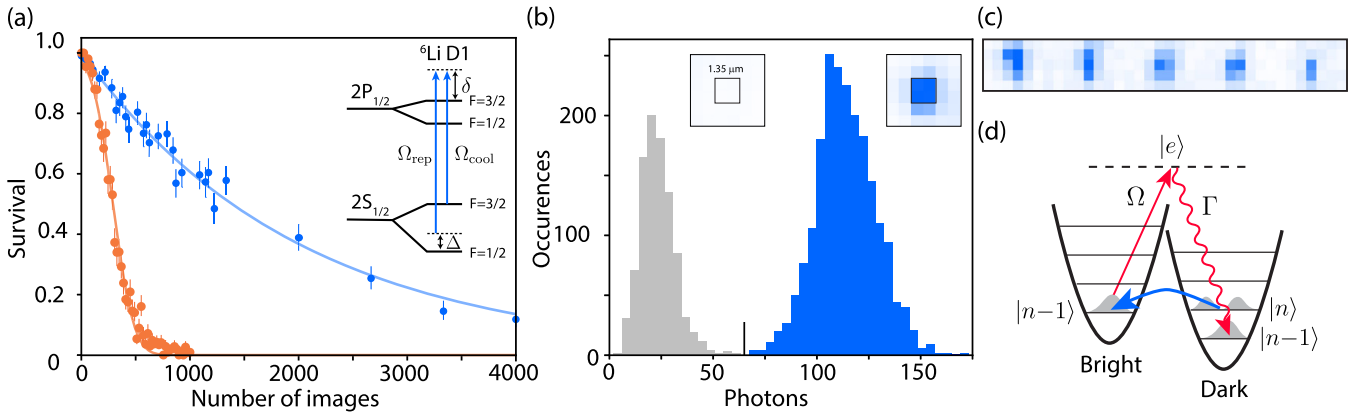


FIG. 1. Low-loss Λ-GM imaging of $^6$Li. (a) Atom survival in an optical tweezer with (blue) and without (orange) active cooling light vs consecutive images. The data with continuous GM cooling have a $1/e$ decay time of 30.0(8) s, corresponding to 2000 images. The atom without active cooling light applied is heated due to off-resonant scattering of the tweezer light and has a $1/e$ time of 5.13(7) s. The inset is the D1 level structure with Λ-GM parameters labeled. (b) Histogram of fluorescence from a single $^6$Li atom trapped in a 1064 nm optical tweezer. This histogram represents an averaged image (3000 shots) of a single region of interest with a signal threshold of 65 photon counts and a loading rate of 0.68(3). Fitting a Gaussian distribution to both peaks and integrating the 0 atom (1 atom) fraction above (below) the signal threshold gives an imaging fidelity of 0.999 7(2). The insets show the cropped region of interest of an image of 0 (left) or 1 (right) atom. (c) Single-shot image of five occupied adjacent tweezer sites. (d) Simplified picture of Λ-GM in a tweezer. A dark state $|D, n\rangle$ couples to the bright state $|B, n-1\rangle$ with one less motional quanta. Spontaneous emission then pumps the population to the dark state $|D, n-1\rangle$ when in the Lamb-Dicke regime.

The tweezer light is split into an array of individual trap sites by an acousto-optic deflector (AOD) before being focused down to the center of our octagon glass cell by a high numerical aperture objective (NA = 0.55). Radial trap frequency measurements in combination with the measured trap depth yield orthogonal radial beam waists of 0.98 and 1.15 μm.

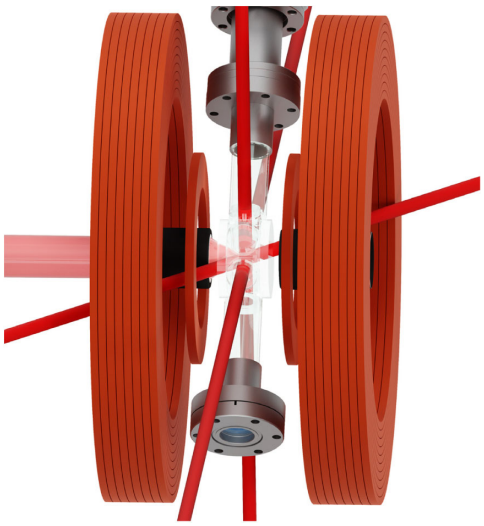

FIG. 2. Single-atom imaging. 1064 nm tweezer light (light red) is focused down to ∼1 μm at the center of the double-sided glass octagon cell. Three retroreflected laser beams containing Λ-GM light (dark red) are sent to the tweezer-trapped atom(s). Fluorescent photons are collected back through the same objective and imaged onto an EMCCD camera. MOT and mini-MOT coils are shown; shim coils are omitted for clarity.

To image $^6$Li in a tweezer, we switch on D1 Λ-GM light for 15 ms and send it through the same path as the three D2 MOT beams, two of which are orthogonal, while one traverses a 30° angle with respect to the tweezer propagation axis (Fig. 2). Scattered 671 nm light is collected through the same objective that the tweezer light is focused through and imaged onto an electron multiplying charge-coupled devices (EMCCD) camera.

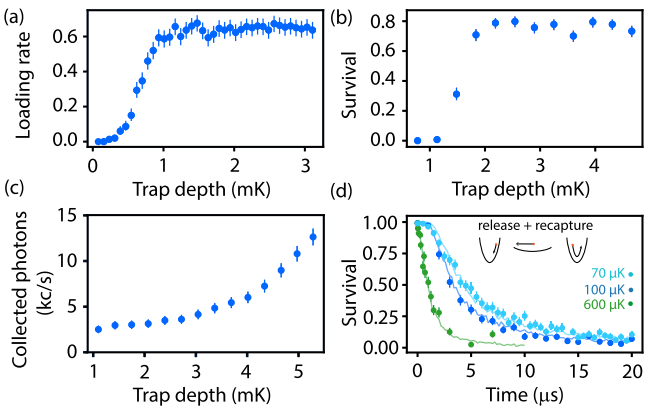


FIG. 3. Properties of $^6$Li in a tweezer. (a) Atom loading vs trap depth (mK). For imaging, trap depth is ramped to a constant value of 3.4 mK. (b) Survival vs trap depth after 533 consecutive image cycles. (c) Photons collected vs trap depth during 15 ms image. In (b) and (c), Λ-GM parameters are not changed as a function of trap depth. (d) Release-and-recapture survival probability under different cooling scenarios. Light blue: optimized cooling for low temperature. Dark blue: optimized cooling for survival. Green: hold in tweezer for 1 s (no cooling light applied). Solid lines are Monte Carlo simulations used to extract a temperature.

Figure 1(b) presents a histogram of collected photons under typical imaging conditions for a single 3.4 mK deep tweezer site. We are able to discriminate between instances of 0 and 1 atom in the tweezer with very high fidelity [0.999 7(2)], as indicated by fitting the bimodal distribution with two Gaussian distributions. Parity projection of the initial Poisson-distributed number of atoms loaded into the trap from several to either 0 or 1 is achieved via an 8 ms light-assisted collision (LAC) pulse. Inspired by the implementation of blue-detuned LAC light in loading rate enhancement beyond the expected stochastic value of 0.5 [16,27–29], we use Λ-GM for our parity projection pulse to achieve loading rates of up to 0.7.

We optimized Λ-GM in the tweezer with respect to either atom survival or temperature. For a 3.4 mK tweezer, we find optimum survival conditions by setting $\Delta = 0$ MHz, $\delta = 20$ MHz, and $I/I_{\mathrm{sat}} = 9.3$. Despite the dark states of the Λ system, we collect photons at our camera at a rate of 6 kc/s resulting in a high imaging fidelity in only 15 ms. This light proved to be more than sufficient for atom imaging [30]. Under survival-optimized conditions, we measure a temperature of 100 μK using the release-and-recapture method [31] [Fig. 3(d), dark blue].

We measure the atom survival under constant application of Λ-GM light. Conditioned on whether an atom was present in the first image, the occupancy of an atom in the second image is counted toward the survival statistics for a given hold time. We plot the survival probability of the atom as a function of imaging cycles in Fig. 1(a). The blue data show the imaging survival versus the number of 15 ms imaging cycles and gives a $1/e$ lifetime of 30.0(8) s, corresponding to 2000 images, or a loss rate per image of 0.000 50(1).

We also measure the atom survival time without any cooling light to obtain a $1/e$ lifetime of 5.13(7) s. Care was taken to ensure that atom loss is not due to the lithium atomic beam or leaked light. This increased loss rate is consistent with heating from the 1064 nm trap laser with an inelastic scattering rate of ∼10 Hz in combination with lithium's large recoil temperature of 3.5 μK. The loss curve fits an error function rather than an exponential, indicating heating. This is evident by measuring an increased temperature of 600 μK after 1 s of simply holding the atom in the tweezer [Fig. 3(d), green].

The lowest temperature reached using Λ-GM in the tweezer is 70 μK, where relative to survival conditions, $\delta$ increased by $\sim\Gamma$, and the cooling and repumper power decrease by a factor of 2 [32].

The imaging survival probability of $^6$Li with Λ-GM cooling is more than an order of magnitude better than previous alkali results in a tweezer. The high fluorescence rate also allows for high imaging fidelity in only 15 ms without additional beams or pulses. To understand this improvement, we simulate Λ-GM cooling for $^6$Li in a harmonic trap by solving the steady-state solution of the full master equation for $^6$Li with both the cooling and repumper beams in $\sigma_+ - \sigma_-$ configuration (detailed further in Supplemental Material [32–34]). Λ-GM has been described by free-space models with classical atoms moving through polarization gradients that vary on the scale of the laser wavelength [35]. The motion of the atom couples the dark states to the bright states, where the atom travels up a potential energy hill before being pumped back to a dark state in a Sisyphus style cooling. This picture works well in free space, but breaks down when the atom is constrained to a length scale much smaller than the wavelength, i.e., when the trapped atom is in the Lamb-Dicke (LD) regime. This discrepancy motivates the development of a new picture of Λ-GM in a tweezer.

The LD parameter [36] is defined as the ratio of the recoil energy to the trapping frequency energy, $\eta_{\mathrm{LD}} = (E_{\mathrm{recoil}}/\hbar\omega)^{1/2} = kx_0$, where $x_0 = \sqrt{\hbar/2m\omega}$ is the ground state harmonic length scale, $k$ is the wave vector of the cooling light, and $\omega$ is the trapping frequency. The atom-field interaction of a plane wave of light in the rotating frame is $H_{\mathrm{AF}} = \Omega\hat{\sigma}^\dagger e^{ik\hat{x}} + \mathrm{H.c.}$, where $\hat{\sigma}$ is the atom lowering operator, and $\hat{x}$ is the atom position operator. In the LD regime, where $\eta_{\mathrm{LD}} \ll 1$, the interaction can be expanded as $H_{\mathrm{AF}} \approx \Omega\hat{\sigma} + \eta_{\mathrm{LD}}\Omega\hat{\sigma}^\dagger(\hat{a} + \hat{a}^\dagger) + \mathrm{H.c.}$, where the zeroth-order term couples states with the same $n$, and the first-order terms couple states with different $n$, resulting in heating or cooling.

Cooling can be understood by the simplified picture shown in Fig. 4(a). When $\Omega_{\mathrm{cool}}$ and $\Omega_{\mathrm{rep}}$ couple the $F = 3/2$ and $F = 1/2$ ground states resonantly ($\Delta = 0$ MHz) with a blue single-photon detuning $\delta$, we can go into a dressed basis of the zeroth-order LD expansion to get bright $|B, n\rangle$ and dark $|D, n\rangle$ states, where $n$ is the harmonic level. The bright states are ac Stark shifted upward by $\Delta E$ due to the blue-detuned light and are coupled to the excited state $|e, n\rangle$ by Ω, while the dark state is not ac Stark shifted or coupled to the excited state. The neighboring motional state $n - 1$ is also drawn and shifted down by the trapping frequency $\hbar\omega$.

The cooling is described in two steps: first [Fig. 4(a), red], spontaneous emission pumps the population from the bright state $|B, n\rangle$ to the dark state $|D, n\rangle$ without changing the motional level; this is followed by a second step [Fig. 4(a), blue], in which the population is transferred from the dark state $|D, n\rangle$ to the bright state $|B, n - 1\rangle$, with a net loss of one motional quanta. Bright or dark state coupling occurs due to the interaction terms $\Omega\hat{\sigma}^\dagger$ and $\eta_{\mathrm{LD}}\Omega\hat{\sigma}^\dagger\hat{a}$, which couple each state to a common excited state $|e, n\rangle$, forming a three-level system in which population is transferred via a coherent Raman transition. The transfer is most efficient when the bright state Stark shift $\Delta E$ is similar to the motional trapping frequency $\hbar\omega$, where the Raman coupling from $|D, n\rangle$ to $|B, n - 1\rangle$ is resonant and strongest. This condition, $\hbar\omega = \Delta E$, is drawn in the simulation Fig. 4(b) as a white dashed line and shows good

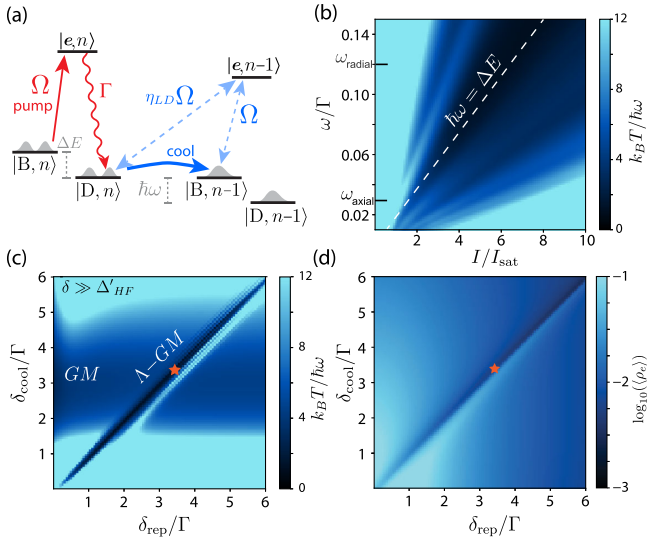


FIG. 4. Simulation of Λ-GM in a tweezer. (a) Λ-GM in a harmonic potential. In step 1, spontaneous emission pumps the bright state $|B,n\rangle$ to the dark state $|D,n\rangle$ with the same motional level. In step 2, the dark state is transferred to the bright state with a net loss of one motional quanta due to the three-level system formed by the Ω and $\eta_{\mathrm{LD}}\Omega$ terms. (b) Simulation of steady-state temperature as a function of cooling power and trapping frequency for $\delta_1 = \delta_2 = 20$ MHz. The dashed line is where the bright state shift equals the trapping frequency. (c) Temperature versus the cooling and repumper detunings. Λ-GM is seen on the diagonal where $\Delta = 0$ MHz. Normal GM is seen away from that condition. (d) Plot of population of steady state in the excited state. The experimental optimum is 0.006 excited, giving a scattering rate consistent with experiment.

agreement with optimal cooling. It also agrees with the criteria from the conventional picture of EIT cooling where the EIT transparency is placed at the $n \to n$ transition and the bright EIT resonance at the $n \to n-1$ transition [37].

Figure 4(b) shows a simulation of the steady-state temperature as a function of cooling power and the trapping frequency $\omega$. The simulation parameters match the experimental settings described above, with $\Omega_{\mathrm{rep}} = \sqrt{0.1}\Omega_{\mathrm{cool}}$, $\delta = 20$ MHz, and $\Delta = 0$ MHz. The temperature is obtained by fitting a Boltzmann distribution to the steady-state motional populations [32]. Similar to the experiment, we find in the simulation that the temperature is lowest for $\Omega_{\mathrm{rep}} \ll \Omega_{\mathrm{cool}}$ because it results in less scattering in the dark states, which, in the limit of low repumper intensity, are just the lower hyperfine states $F = 1/2$. The axial and radial trapping frequencies are marked on the $y$ axis. The simulated temperatures are 41 μK for radial and 82 μK for axial, where the summed averaged energies results in a temperature of 92 μK, in good agreement with the measured release-and-recapture temperature. These temperatures correspond to 43% and 11% motional ground state population for the radial and axial dimensions, respectively.

Crucially, we see that the axial and radial cooling have different optimal conditions. Experimentally, we have optimized the combined temperature, but the simulation suggests we could cool further by pulsing the radial and axial cooling separately with different powers and detunings.

In Fig. 4(c), we plot the radial temperature as a function of the two single-photon detunings, with $I/I_{\mathrm{sat}} = 6$. The star marks the experimentally determined survival optimum. The simulation shows gray molasses (GM) cooling centered around $\delta_{\mathrm{cool}} \approx 3\Gamma$, where it decays as the detuning increases beyond the excited-state hyperfine splitting of 26 MHz where the tensor shift is canceled out by the coupling to both excited hyperfine states. Notably, GM is largely insensitive to the detuning of the low-intensity repumper laser. Λ enhancement is found along the diagonal where $\Delta \approx 0$ MHz, where a corresponding factor of 2 decrease in temperature is predicted relative to standard GM.

Figure 4(d) plots the excited state population of the steady-state solution from Fig. 4(c). The simulation predicts a total scattering rate of 220 kc/s, in good agreement with our collected photon rate of 6 kc/s and a collection efficiency predicted to be ∼3%. We also find an explanation for why lithium Λ-GM in a tweezer is relatively bright—the small excited hyperfine splitting ruins the three-level system model and prevents the dark state from becoming greater than 99.5% dark under any conditions.

In conclusion, we have loaded lithium-6 directly from a MOT into optical tweezers with an enhanced loading rate in 100 ms. Individual lithium atoms have been imaged thousands of times with Λ-enhanced gray molasses light, where, despite its light mass, high recoil energy, and a lack of accessible narrow lines, we obtain a survival probability of 0.999 50(2), which sets the benchmark for low-loss neutral atom imaging in a tweezer. Additionally, an imaging fidelity of 0.999 7(2) improves upon existing lithium single atom imaging by an order of magnitude.

We have simultaneously developed a model that describes Λ-GM in the tweezer, which accurately predicts scattering rate and steady-state temperature. The order of magnitude improvement for tweezer imaging survival and excellent agreement between simulation and experimental results also instills optimism for exploring enhanced cooling methods for other alkali atoms. Our model elucidates new strategies for motional cooling in the tweezer, which could pave the way toward ground state preparation of lithium as a prelude to LiCs molecular assembly.

We thank Ben Cerjan, Phil Wyss, Mark Carlsen, and the Jonathan Amy Facility for Chemical Instrumentation for valuable contributions to the instrumentation. This work was supported by the NSF Career Award (Award No. 0543784).

*hoodjd@purdue.edu


[1] A. Kaufman, B. Lester, C. Reynolds, M. Wall, M. Foss-Feig, K. Hazzard, A. Rey, and C. Regal, Science **345**, 306 (2014).

[2] B. M. Spar, E. Guardado-Sanchez, S. Chi, Z. Z. Yan, and W. S. Bakr, Phys. Rev. Lett. **128**, 223202 (2022).

[3] H. Levine, A. Keesling, A. Omran, H. Bernien, S. Schwartz, A. S. Zibrov, M. Endres, M. Greiner, V. Vuletić, and M. D. Lukin, Phys. Rev. Lett. **121**, 123603 (2018).

[4] S. Ma, A. P. Burgers, G. Liu, J. Wilson, B. Zhang, and J. D. Thompson, Phys. Rev. X **12**, 021028 (2022).

[5] L. R. Liu, J. D. Hood, Y. Yu, J. T. Zhang, K. Wang, Y.-W. Lin, T. Rosenband, and K.-K. Ni, Phys. Rev. X **9**, 021039 (2019).

[6] S. Spence, R. Brooks, D. Ruttley, A. Guttridge, and S. L. Cornish, New J. Phys. **24**, 103022 (2022).

[7] K. Wang, X. He, R. Guo, P. Xu, C. Sheng, J. Zhuang, Z. Xiong, M. Liu, J. Wang, and M. Zhan, Phys. Rev. A **100**, 063429 (2019).

[8] J. T. Zhang, Y. Yu, W. B. Cairncross, K. Wang, L. R. B. Picard, J. D. Hood, Y.-W. Lin, J. M. Hutson, and K.-K. Ni, Phys. Rev. Lett. **124**, 253401 (2020).

[9] C. M. Holland, Y. Lu, and L. W. Cheuk, arXiv:2210.06309.

[10] Y. Bao, S. S. Yu, L. Anderegg, E. Chae, W. Ketterle, K.-K. Ni, and J. M. Doyle, arXiv:2211.09780.

[11] M. Endres, H. Bernien, A. Keesling, H. Levine, E. R. Anschuetz, A. Krajenbrink, C. Senko, V. Vuletic, M. Greiner, and M. D. Lukin, Science **354**, 1024 (2016).

[12] D. Barredo, V. Lienhard, S. De Leseleuc, T. Lahaye, and A. Browaeys, Nature (London) **561**, 79 (2018).

[13] L. Liu, J. Hood, Y. Yu, J. Zhang, N. Hutzler, T. Rosenband, and K.-K. Ni, Science **360**, 900 (2018).

[14] Y. Yu, N. R. Hutzler, J. T. Zhang, L. R. Liu, J. D. Hood, T. Rosenband, and K.-K. Ni, Phys. Rev. A **97**, 063423 (2018).

[15] A. T. Grier, I. Ferrier-Barbut, B. S. Rem, M. Delehaye, L. Khaykovich, F. Chevy, and C. Salomon, Phys. Rev. A **87**, 063411 (2013).

[16] J. Ang'ong'a, C. Huang, J. P. Covey, and B. Gadway, Phys. Rev. Res. **4**, 013240 (2022).

[17] D. Boiron, A. Michaud, P. Lemonde, Y. Castin, C. Salomon, S. Weyers, K. Szymaniec, L. Cognet, and A. Clairon, Phys. Rev. A **53**, R3734 (1996).

[18] A. Burchianti, G. Valtolina, J. A. Seman, E. Pace, M. De Pas, M. Inguscio, M. Zaccanti, and G. Roati, Phys. Rev. A **90**, 043408 (2014).

[19] C. F. Roos, D. Leibfried, A. Mundt, F. Schmidt-Kaler, J. Eschner, and R. Blatt, Phys. Rev. Lett. **85**, 5547 (2000).

[20] E. Haller, J. Hudson, A. Kelly, D. A. Cotta, B. Peaudecerf, G. D. Bruce, and S. Kuhr, Nat. Phys. **11**, 738 (2015).

[21] G. J. A. Edge, R. Anderson, D. Jervis, D. C. McKay, R. Day, S. Trotzky, and J. H. Thywissen, Phys. Rev. A **92**, 063406 (2015).

[22] J. P. Covey, I. S. Madjarov, A. Cooper, and M. Endres, Phys. Rev. Lett. **122**, 173201 (2019).

[23] M. F. Parsons, A. Mazurenko, C. S. Chiu, G. Ji, D. Greif, and M. Greiner, Science **353**, 1253 (2016).

[24] P. T. Brown, D. Mitra, E. Guardado-Sanchez, P. Schauß, S. S. Kondov, E. Khatami, T. Paiva, N. Trivedi, D. A. Huse, and W. S. Bakr, Science **357**, 1385 (2017).

[25] A. Bergschneider, V. M. Klinkhamer, J. H. Becher, R. Klemt, G. Zürn, P. M. Preiss, and S. Jochim, Phys. Rev. A **97**, 063613 (2018).

[26] M. Holten, L. Bayha, K. Subramanian, C. Heintze, P. M. Preiss, and S. Jochim, Phys. Rev. Lett. **126**, 020401 (2021).

[27] M. O. Brown, T. Thiele, C. Kiehl, T.-W. Hsu, and C. A. Regal, Phys. Rev. X **9**, 011057 (2019).

[28] T. Grünzweig, A. Hilliard, M. McGovern, and M. Andersen, Nat. Phys. **6**, 951 (2010).

[29] B. J. Lester, N. Luick, A. M. Kaufman, C. M. Reynolds, and C. A. Regal, Phys. Rev. Lett. **115**, 073003 (2015).

[30] L. W. Cheuk, L. Anderegg, B. L. Augenbraun, Y. Bao, S. Burchesky, W. Ketterle, and J. M. Doyle, Phys. Rev. Lett. **121**, 083201 (2018).

[31] C. Tuchendler, A. M. Lance, A. Browaeys, Y. R. P. Sortais, and P. Grangier, Phys. Rev. A **78**, 033425 (2008).

[32] See Supplemental Material at http://link.aps.org/supplemental/10.1103/PhysRevLett.131.083001 for experimental data and tweezer cooling simulations.

[33] M. E. Gehm, Properties of $^6$Li, https://jet.physics.ncsu.edu/techdocs/pdf/PropertiesOfLi.pdf (accessed: 2023-04-28).

[34] D. A. Steck, Quantum, atom optics, available online at http://steck.us/teaching (revision 0.13.19, 6 April 2023) (2023).

[35] G. Salomon, L. Fouché, P. Wang, A. Aspect, P. Bouyer, and T. Bourdel, Europhys. Lett. **104**, 63002 (2014).

[36] D. Leibfried, R. Blatt, C. Monroe, and D. Wineland, Rev. Mod. Phys. **75**, 281 (2003).

[37] G. Morigi, J. Eschner, and C. H. Keitel, Phys. Rev. Lett. **85**, 4458 (2000).